Fractal and subharmonic responses driven by surface acoustic waves during charge density wave sliding

Yu Funami ● and Kazushi Aoyama

Department of Earth and Space Science, Graduate School of Science, Osaka University, Osaka 560-0043, Japan

We theoretically investigate the effects of surface acoustic waves (SAWs) on an electric-field-driven sliding motion of a one-dimensional charge density wave (CDW), which is initially pinned by impurities. By numerically analyzing an extended Fukuyama-Lee-Rice model, we show that a mechanical vibration of the SAW, which, in the model, is assumed to affect the CDW via the pinning site in the form of temporally oscillating pinning parameters, induces Shapiro steps with self-similarity, i.e., the devil's staircase, in the current-voltage characteristics. It is also found that when the SAW acts as the vibration in the pinning strength, the mechanism of the mode locking (harmonic and subharmonic responses) leading to the occurrence of the Shapiro steps is modified, and as a result, the fractal dimension and parameter dependence of the SAW-induced staircase can be considerably different from those for the conventional ac-electric-field-induced one. This suggests that an unconventional type of fractal phenomena can emerge in the SAW-induced CDW dynamics.

Fractals with their characteristic properties exemplified by self-similarity and noninteger dimensions often appear in nature in various forms such as coastlines, snowflakes, and polymer chains [1,2]. Of particular interest are fractal phenomena induced by dynamical effects, one example of which is a sliding motion of a charge density wave (CDW), an electron condensate emerging typically in quasi-one-dimensional conductors such as $NbSe_3$, TaS_3, and $K_{0.3}MoO_3$ [3–5]. When the one-dimensional CDW is driven to slide by an external dc electric field E_{dc} [6–8], an electric current carried by the sliding CDW I_{CDW} as a function of E_{dc}, i.e., the *I-V* characteristics, is known to exhibit step-like fractal structures, the so-called devil's staircase, in the presence of an additional ac electric field E_{ac} [9–12]. Subharmonic responses emerging in the staircase as fractional-value plateaus are closely related to time crystals in periodically driven systems [13]. In this Letter, motivated by recent experiments where mechanical vibrations [14] including a surface acoustic wave (SAW) [15] were applied instead of E_{ac}, we theoretically investigate vibration effects on the staircase formation in the CDW sliding.

The CDW state is characterized by a spatial modulation in the electron density, which, in one dimension, takes the following form:

$$\rho(x,t) = \rho_0 + \rho_1 \cos[\phi(x,t) + Qx]. \quad (1)$$

Here, ρ_0 is the average electron density, and ρ_1 and Q are, respectively, the amplitude and wave number of the CDW modulation whose phase $\phi(x,t)$ plays an important role for the CDW dynamics. In materials, the CDW modulation is locally deformed due to impurities, defects, and lattice distortions, which can be described as a pinning of the CDW phase ϕ [18,19]. Such a pinned object can be driven by an external force overcoming an associated static friction [20,21], which, in the present CDW case, is an external electric field E. When the dc component of E, E_{dc}, exceeds a threshold value, the

CDW is depinned and begins to slide with velocity $v = \frac{1}{Q}\frac{d\phi}{dt}$, carrying the associated current I_{CDW} proportional to $v = \frac{1}{Q}\frac{d\phi}{dt}$ [3,4,6–8]. In this sliding regime, there exists a characteristic frequency ω_ϕ, the so-called narrow band noise [22,23], which corresponds to a period for a specific part of the CDW, e.g., the peak position of the wave, to pass through a fixed pinning site, and thus is given by $\omega_\phi = vQ = \frac{d\phi}{dt}$. This oscillating mode ω_ϕ is related to I_{CDW} via

$$I_{CDW} \propto \frac{d\phi}{dt} = \omega_\phi. \quad (2)$$

In the case without the ac component ($E_{ac} = 0$), I_{CDW}, or equivalently, ω_ϕ, gradually increases with increasing the driving force E_{dc}.

When the dc and ac fields are simultaneously applied, i.e., $E = E_{dc} + E_{ac}\sin(\omega_{ex}t)$, the sliding mode ω_ϕ is coupled to the external frequency ω_{ex}, leading to the emergence of plateau regions in the *I-V* characteristics [9–11,24–35]. A typical theoretical result is shown in Fig. 1(a). The plateaus where ω_ϕ is mode-locked to $\omega_\phi = (p/q)\omega_{ex}$ with integers p and q are CDW analog of the Shapiro steps discussed in the context of superconductivity [36–38]. The plateaus with integer values of p/q are called harmonic steps and others are called subharmonic steps. In the overdamped regime, the former can be explained by a single-impurity model, whereas the latter, corresponding to discrete-time-crystal states [13], can be explained by many-body multi-impurity models [3]. One can see from Fig. 1(a) that so many subharmonic steps construct a self-similar structure in the *I-V* characteristics. Although, in general, the occurrences of the subharmonic steps and the devil's staircase are not equivalent, the fractal nature has been confirmed in theoretical works [3,11,29,39] and in one experiment as well [9]. The E_{ac}-driven staircase is

(a) ac-electric-field case
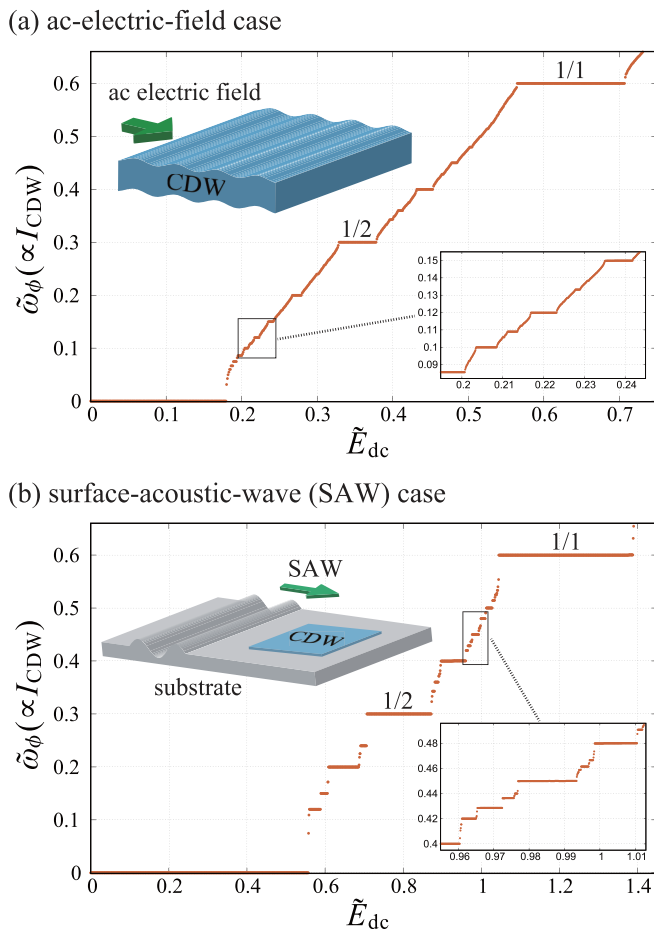

(b) surface-acoustic-wave (SAW) case

FIG. 1. The $\tilde{E}_{dc}$ dependence of $\tilde{\omega}_\phi$ (the I-V characteristics) in (a) the ac-electric-field case of $\tilde{E}_{ac} = 3.0$, $\tilde{P}_{dc} = 2.0$, and $\tilde{P}_{ac} = 0$ and (b) the SAW case of $\tilde{E}_{ac} = 0$, $\tilde{P}_{dc} = 2.0$, and $\tilde{P}_{ac} = 1.2$, where the results are obtained for $\tilde{\omega}_{ex} = 0.6$ and $N_{imp} = 200$. In each figure, the inset shows a magnified view of a small area enclosed by a box and the top left image shows the system setup in each case.

considered to belong to the universality class of the circle map where the fractal dimension is $D = 0.87$ [10,12].

Quite recently, the Shapiro steps have also been observed in a different kind of experiment where, instead of E_{ac}, a time-dependent strain [14] was applied. In addition, the effect of another type of mechanical force, the SAW, on CDW sliding has also been reported [15], though in this case, an electrical contribution as well as the mechanical one might be relevant. In contrast to the electromagnetic interaction between E_{ac} and CDW, how the mechanical forces affect CDW is an interesting issue. In this work, assuming that the mechanical vibration indirectly interacts with the CDW via the pinning sites, we theoretically investigate its effect on the CDW dynamics. We mainly focus on the SAW case with presumably spatially nonuniform strains as a typical platform for a pinning-strength vibration (see Sec. I in [40]), which is a key ingredient for the following results. We will show that the pinning-strength vibration caused by the SAW induces Shapiro steps with a nontrivial fractal dimension and a parameter dependence of the step width which is qualitatively different from the E_{ac}-induced one.

Although even the threshold-field physics cannot fully be explained by a compact theory [48], many aspects of the CDW sliding can be described by the Fukuyama-Lee-Rice model [49–51] whose overdamped equation of motion in one dimension is given by

$$\left(\gamma \frac{\partial}{\partial t} - v_{ph}^2 \nabla^2\right)\phi = P_{imp}N_p(x)\sin(\phi + Qx) + \frac{eQ}{m^*}E, \quad (3)$$

where e, m^*, and v_{ph} are the electric charge, the effective mass of the CDW, and the phason velocity, respectively, and γ is the phenomenologically introduced damping constant. In the first term on the right-hand side of Eq. (3), P_{imp} represents the pinning strength and $N_p(x) = \sum_{i=1}^{N_{imp}} \delta(x - R_i)$ is the distribution function of pinning sites whose positions and total number are denoted by R_i and N_{imp}, respectively, where we assume, for simplicity, that the pinning strength does not depend on the pinning-site position. In the usual case without the SAW, both P_{imp} and R_i are static constants, and the electric field $E = E_{dc} + E_{ac}\sin(\omega_{ex}t)$ gives rise to the nonlinear CDW dynamics. In the presence of the SAW, however, P_{imp} and R_i would not be static constants any more, as explained below.

In the SAW experiment shown in the image of Fig. 1(b), the substrate oscillation driven by the SAW with frequency ω_{ex} should more or less propagate into the CDW, shaking the pinning position and strength with frequency ω_{ex} [41,42,52]. Since the ω_{ex}-dependent "pinning-position" vibration turns out to play essentially the same role as E_{ac} [40,42] (in [41] treating a similar situation, due to a single-impurity assumption and a truncation of the nonlinear effect, results different from those in [40,42] are obtained), here, we consider the ω_{ex}-dependent "pinning-strength" of the form $P_{imp}(t) = P_{dc} + P_{ac}\sin(\omega_{ex}t)$, which could be caused by, for example, strain-induced parameter changes [44] and the influences of nonuniform strains on the effective pinning [40]. In the presence of this temporally periodic pinning force $P_{imp}(t)$, we switch on E_{dc} to drive the sliding motion of the CDW with E_{ac} remaining off.

Since Eq. (3) cannot be solved analytically due to the nonlinear pinning force, we numerically solve Eq. (3), which can be rewritten in the dimensionless form as

$$\frac{d\phi_i}{d\tilde{t}} - (\phi_{i+1} - 2\phi_i + \phi_{i-1}) = \tilde{P}_{imp}\sin(\phi_i + \beta_i) + \tilde{E}. \quad (4)$$

The spatial coordinate is discretized in units of a length scale l, which can be either the mean impurity distance [26,31] or the phase correlation length, and β_i involving the randomly distributed R_i is a random number between 0 and 2π (for details, see Sec. I in [40]). Other dimensionless quantities are defined by $\tilde{t} = t/[(\gamma l_{imp}^2)/v_{ph}^2]$, $\tilde{E} = (eQl_{imp}^2/m^*v_{ph}^2)E$, and $\tilde{P}_{imp} = (l_{imp}^2/v_{ph}^2)P_{imp}$. Then, the CDW current [see Eq. (2)] averaged over space and time is given by $I_{CDW} \propto \frac{1}{N_{imp}} \sum_{i=1}^{N_{imp}} \langle\frac{d\phi_i}{d\tilde{t}}\rangle_{\tilde{t}} = \tilde{\omega}_\phi$, where $\langle\rangle_{\tilde{t}}$ denotes the time average. We note that a nonlinear equation analogous to Eq. (4) appears in the Frenkel-Kontorova (FK) model [39,42,53,54] to which the following results could be applied when the FK-potential depth vibrates.

By using the fourth-order Runge-Kutta method with a random initial configuration for ϕ_i and time step $\Delta\tilde{t} = 0.1$,
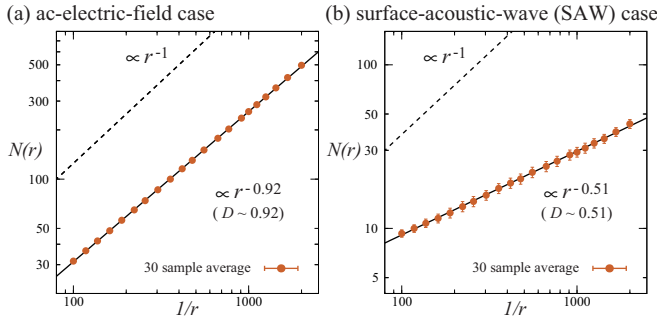
FIG. 2. The log-log plot of $N(r)$ as a function of $1/r$ in the (a) ac-electric-field and (b) SAW cases, where the same parameters as those in Fig. 1 are used. Solid lines indicate power-law functions of the from $(1/r)^D$ with (a) $D \sim 0.92$ and (b) $D \sim 0.51$, which are obtained by fitting the numerical data. For comparison, the slope in the trivial case of $D = 1$ is also shown.
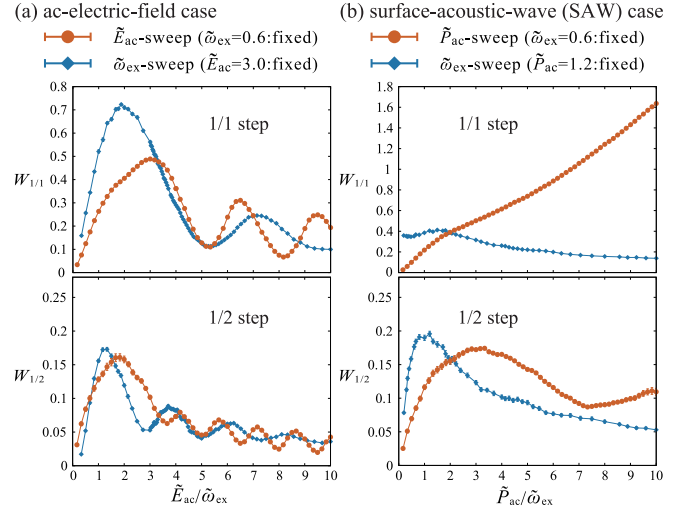

FIG. 3. The parameter dependence of the harmonic 1/1-step width $W_{1/1}$ (upper panels) and the subharmonic 1/2-step width $W_{1/2}$ (lower panels) in the (a) ac-electric-field and (b) the SAW cases. In (a) [(b)], the horizontal axis denotes $\tilde{E}_{ac}/\tilde{\omega}_{ex}$ ($\tilde{P}_{ac}/\tilde{\omega}_{ex}$), and red and blue symbols represent the $\tilde{E}_{ac}$ ($\tilde{P}_{ac}$) dependence at $\tilde{\omega}_{ex} = 0.6$ and the $\tilde{\omega}_{ex}$ dependence at $\tilde{E}_{ac} = 3.0$ ($\tilde{P}_{ac} = 1.2$), respectively.

we integrate Eq. (4) typically up to $\tilde{t} = 2.0 \times 10^5$, where the first 10^4 time steps are discarded for relaxation. Although the total number of impurities is fixed to be $N_{imp} = 200$, we have made spot checks that results for $N_{imp} = 200$ and 400 are unchanged. The random average over the impurity distributions corresponding to the β_i configurations is taken over 30 samples. We calculate $\tilde{\omega}_\phi \propto I_{CDW}$ in two cases, the ac-electric-field case of $\tilde{E} = \tilde{E}_{dc} + \tilde{E}_{ac} \sin(\tilde{\omega}_{ex}\tilde{t})$ and $\tilde{P}_{imp} = \tilde{P}_{dc}$ and the SAW case of $\tilde{E} = \tilde{E}_{dc}$ and $\tilde{P}_{imp} = \tilde{P}_{dc} + \tilde{P}_{ac} \sin(\tilde{\omega}_{ex}\tilde{t})$. The former is mainly for reference. Throughout this paper, $\tilde{P}_{dc} = 2.0$ and $\tilde{\omega}_{ex} = 0.6$ are basically used.

Figure 1 shows a typical example of the $\tilde{E}_{dc}$ dependence of $\tilde{\omega}_\phi$, i.e., the I-V characteristic, for a fixed β_i configuration in Fig. 1(a) the ac-electric-field case of $\tilde{E}_{ac} = 3.0$ and $\tilde{P}_{ac} = 0$ and Fig. 1(b) the SAW case of $\tilde{E}_{ac} = 0$ and $\tilde{P}_{ac} = 1.2$. As readily seen from the main panel of Fig. 1(b), the Shapiro steps appear in the SAW case, as in the well-known case of the ac electric field shown in Fig. 1(a). The harmonic and subharmonic steps can be identified from the relation $\tilde{\omega}_\phi = (p/q)\tilde{\omega}_{ex}$. In the case of Fig. 1 where the external frequency is fixed to be $\tilde{\omega}_{ex} = 0.6$, the plateau at $\tilde{\omega}_\phi = 0.6$ corresponds to the 1/1 harmonic step of $p = 1$ and $q = 1$, and subharmonic steps with noninteger values of p/q such as the 1/2 step of $p = 1$ and $q = 2$ corresponding to $\tilde{\omega}_{ex} = 0.3$ can be identified in the same manner. We note that the 0/1 harmonic step corresponds to the non-sliding region of $\tilde{\omega}_\phi = 0$. In each of Figs. 1(a) and 1(b), consecutive subharmonic steps in a small $\tilde{E}_{dc}$ window (see the magnified view shown in the inset) construct a structure similar to the entire staircase over the wide $\tilde{E}_{dc}$ region. A fractal structure characterized by self-similarity of this kind is known as the devil's staircase.

To check the fractal nature of the Shapiro steps, we calculate the fractal dimension D in the same manner as that in [10,11]. In the $\tilde{E}_{dc}$ region between the 0/1 and 1/1 steps (suppose that l is the width of this region), we first count the total width $S(r)$ of steps that are larger than an arbitrarily taken stepwidth r, and then, calculate a function $N(r) = [l - S(r)]/r$, which, for the devil's staircase, should behave as $N(r) \propto (1/r)^D$ in the $r \to 0$ limit. We note that in the absence of the subharmonic steps as in the single impurity model, the

fractal dimension D is trivially 1 and that the deviation of the D value from 1 points to the emergence of the fractal nature in the staircase involving the subharmonic steps. Figure 2 shows the log-log plots of $N(r)$ as a function of $1/r$ in the [Fig. 2(a)] ac-electric-field and [Fig. 2(b)] SAW cases, where in counting $S(r)$, we regard a plateau whose $\tilde{\omega}_\phi$ is unchanged within a precision of the order of 10^{-4} as a single Shapiro step. As one can see from Fig. 2, the $N(r)$'s in both cases linearly increase toward $\frac{1}{r} \to \infty$ ($r \to 0$) in the log-log plot, suggestive of the fractal behavior $N(r) \propto (1/r)^D$. Actually, the numerical data can be well fitted by power-law functions of the form $a(1/r)^D$, where the fractal dimensions are obtained as $D \sim 0.92$ and $D \sim 0.51$ in the ac-electric-field and SAW cases, respectively. Although the D values depend on the system parameters as reported for a similar model [39], the former is close to the experimental value of $D \sim 0.91$ obtained for the ac electric field [9] and the theoretical universal value of $D = 0.87$ for the circle map [10,11]. The latter value of $D \sim 0.51$, on the other hand, is much smaller than the two above values, indicating that the mechanisms of the step formation, i.e., the mode locking, in the ac-electric-field and SAW cases are different. To see the possible difference in the mode-locking likely relevant to the fractal nature, we next examine the parameter dependence of the Shapiro step width.

Figures 3(a) and 3(b) show the parameter dependence of the 1/1 harmonic step width $W_{1/1}$ and the 1/2 subharmonic one $W_{1/2}$ in the ac-electric-field and SAW cases, respectively ($W_{0/1}$ data are also available in [40]), where red (blue) symbols are obtained by changing the amplitude (frequency) of the time-varying external field with the frequency (amplitude) being fixed. Although the larger $\tilde{P}_{ac}$ region of $\tilde{P}_{ac} > \tilde{P}_{dc}$ might be unrealistic, we present the data just for comparison with Fig. 3(a). In the ac-electric-field case shown in Fig. 3(a), the harmonic step width $W_{1/1}$ (see the upper panel) exhibits a damping oscillation with increasing $\tilde{E}_{ac}$ or $1/\tilde{\omega}_{ex}$ as

reported elsewhere [25,45,47,53,55], and such a situation is also the case for the subharmonic-step width [54] (see the lower panel). In the SAW case shown in Fig. 3(b), on the other hand, $W_{1/1}$ monotonically increases with increasing the amplitude $\tilde{P}_{ac}$, whereas it is almost independent of the external frequency $\tilde{\omega}_{ex}$, suggesting that the 1/1 step is robust against higher-frequency SAW. The subharmonic step width $W_{1/2}$ also does not show an oscillating behavior as a function of $\frac{\tilde{P}_{ac}}{\tilde{\omega}_{ex}}$. The difference can intuitively be understood by a washboard description where the swing of a particle between potential local maxima is essential for the oscillation valleys of $W_{1/1}$ [55]. Since the swing is caused by the periodic driving force E_{ac}, $W_{1/1}$ shows no oscillation in the SAW case of $E_{ac} = 0$ where the SAW corresponds to a vibration of the potential depth, i.e., a vertical motion in the washboard description, and such a situation should also be the case for other nondriving vertical vibrations.

To further examine how the CDW mode ω_ϕ is coupled to the external frequency ω_{ex}, we perform the perturbative calculation proposed in [32] (for details of the following calculation, see Sec. IV in [40]). Assuming that the CDW phase takes the form of $\phi(x, t) = \phi_0(t) + \delta\phi(x, t)$ with the globally sliding mode $\phi_0(t) = \omega_\phi t - \frac{\overline{E}_{ac}}{\omega_{ex}} \cos(\omega_{ex} t)$ and local deviation $\delta\phi(x, t)$, we self-consistently determine ω_ϕ. For later convenience, the electric field E is normalized as $\overline{E} = \left(\frac{eQ}{\gamma m^*}\right) E$. By substituting the above expression for $\phi(x, t)$ into Eq. (3), we obtain

$$\delta\phi(x, t) = \frac{1}{v_{ph}^2} \int dx' dt' \tilde{G}(x - x', t - t') E_P[x', \phi(x', t')],$$
$$(5)$$

$$\omega_\phi = \frac{1}{\gamma} \langle E_P[x, \phi(x, t)] \rangle_{x,t} + \overline{E}_{dc},$$
$$(6)$$

with the pinning term

$$E_P[x, \phi(x, t)] = P_{imp} N_p(x) \sin[\phi_0(t) + \delta\phi(x, t) + Qx], \quad (7)$$

where $\langle \rangle_{x,t}$ denotes the average over space and time and $\tilde{G}(x, t) = G(x, t) - \langle G(x, t) \rangle_{x,t}$ with the Green's function G satisfying $\left(\frac{\gamma}{v_{ph}^2} \frac{\partial}{\partial t} - \nabla^2\right) G(x, t) = \delta(x)\delta(t)$. As $E_P[x, \phi(x, t)]$ involves ω_ϕ via $\phi_0(t)$, Eq. (6) turns out to be the self-consistent equation for ω_ϕ. By using the expansion with respect to $\delta\phi$, $E_P = P_{imp} N_p(x)\{\sin[\phi_0(t) + Qx] + \cos[\phi_0(t) + Qx]\delta\phi + \cdots\}$, we can solve Eq. (5) successively to obtain $\delta\phi(x, t)$, which will further be substituted into Eq. (6) to determine ω_ϕ. Noting that $N_P(x)$ represents the random impurity distribution, the leading-order contribution to $\langle E_P[x, \phi(x, t)] \rangle_{x,t}$ turns out to be of second order in P_{imp}, and is given by

$$E_P^{(2)}(\omega_\phi) \propto \int dt \, dt' P_{imp}(t) P_{imp}(t') \tilde{G}(0, t - t')$$
$$\times \sin[\phi_0(t) - \phi_0(t')]. \quad (8)$$

In the ac-electric-field case of $E_{ac} \neq 0$ and $P_{imp} = P_{dc}$, ω_ϕ and ω_{ex} are coupled in the $\sin[\phi_0(t) - \phi_0(t')]$ part in Eq. (8),

which contains

$$e^{i\phi_0(t)} = e^{i[\omega_\phi t - \frac{\overline{E}_{ac}}{\omega_{ex}} \cos(\omega_{ex} t)]} = \sum_p (-i)^p J_p\left(\frac{\overline{E}_{ac}}{\omega_{ex}}\right) e^{i(\omega_\phi - p\omega_{ex})t},$$
$$(9)$$

with the Bessel function $J_p(x)$. Thus, we have

$$E_P^{(2)}(\omega_\phi) \propto P_{dc}^2 \sum_p J_p^2\left(\frac{\overline{E}_{ac}}{\omega_{ex}}\right) \text{Im}[\tilde{H}(\omega_\phi - p\,\omega_{ex})], \quad (10)$$

where $\tilde{H}(\omega) = \int \frac{dk}{2\pi} \tilde{G}(k, \omega)$ is a function diverging at $\omega = 0$ [31,40]. Since $E_P^{(2)}(\omega_\phi)$ increases to diverge at $\omega_\phi - p\omega_{ex} = 0$, the solution of Eq. (6) is definitely $\omega_\phi = p\omega_{ex}$, which corresponds to the $p/1$ harmonic step. Since the coefficient $P_{dc}^2 \sum_p J_p^2\left(\frac{\overline{E}_{ac}}{\omega_{ex}}\right)$ is related to the robustness of the solution against $\overline{E}_{dc}$, it should determine the step width, as it can be inferred from the Bessel-function-like oscillating behavior of the step width as a function of $\frac{\overline{E}_{ac}}{\omega_{ex}}$ [see Fig. 3(a)]. We note that higher-order contributions are relevant to subharmonic steps [31].

In the SAW case of $E_{ac} = 0$ and $P_{imp} = P_{dc} + P_{ac} \sin(\omega_{ex} t)$, $P_{imp}(t) P_{imp}(t') \sin[\phi_0(t) - \phi_0(t')]$ in Eq. (8) yields the ω_ϕ-ω_{ex} coupling of the form

$$P_{imp}(t) e^{i\phi_0(t)} = P_{dc} e^{i\omega_\phi t} + \frac{P_{ac}}{2i}[e^{i(\omega_\phi + \omega_{ex})t} - e^{i(\omega_\phi - \omega_{ex})t}]. \quad (11)$$

In contrast to the ac-electric-field case where the global vibration of the CDW [the oscillating part in $\phi_0(t)$] is indirectly coupled to ω_ϕ via the pinning site [see Eq. (9)], the pinning-site vibration of the SAW directly acts on ω_ϕ [see Eq. (11)]. Then, $E_P^{(2)}(\omega_\phi)$ is calculated as

$$E_P^{(2)}(\omega_\phi) \propto \text{Im}\left[P_{dc}^2 \tilde{H}(\omega_\phi) + \frac{P_{ac}^2}{4} \sum_{p=\pm 1} \tilde{H}(\omega_\phi - p\,\omega_{ex})\right].$$
$$(12)$$

Due to the direct ω_ϕ-ω_{ex} coupling, ω_{ex} appears only in $\tilde{H}(\omega)$ yielding the mode-locking condition for the 1/1 step, and its step width determined by the coefficient of $\tilde{H}(\omega)$ becomes an ω_{ex}-independent increasing function of P_{ac}, being consistent with the numerical result shown in the top panel of Fig. 3(b). The direct coupling process of Eq. (11) works also in higher-order contributions relevant to other steps including the subharmonic ones, so that the Bessel-function-like oscillating behavior does not appear in the SAW case. The analytical result presented here, i.e., Eq. (12) [Eq. (10)], is consistent with the numerical result shown in Fig. 3(b) [Fig. 3(a)], which suggests that the mode-locking in the SAW case (the ac-electric-field case) is direct (indirect). Such a qualitative difference in the step formation, i.e., whether the mode locking is direct or indirect, could also affect the entire structure of the staircase, eventually leading to the difference in the fractal dimension as demonstrated in Fig. 2.

In this work, we investigated the effect of the SAW on the overdamped sliding motion of the CDW, assuming that the SAW affects the CDW via pinning sites, where importantly, the pinning-strength vibration P_{ac} induces the unconventional direct mode-locking distinct from the E_{ac}-induced indirect

one. In the associated experiments, the impurity-position vibration [40–42] may also be relevant, and the SAW generated in the piezoelectric substrate may inversely yield an electric field by the piezoelectric effect. In addition, the SAW frequency of the order of a few GHz is below but not so far from values typical of the underdamped CDW motion [23,56–59] in which a $\frac{\partial^2}{\partial t^2}\phi$ term dropped in Eq. (3) becomes important. These elements which are not taken into account in this work might be relevant to the CDW dynamics in the presence of the SAW, but experimental data enabling us to discuss them are yet to be reported. Although the validity of the simplified modeling used here should carefully be assessed by

analyzing the fractal dimension and the parameter dependence of the step width in future experimental works, we believe that this work presenting the unconventional mode-locking mechanism will promote the exploration of new classes of fractal phenomena and periodically driven systems.

[1] B. B. Mandelbrot, *The Fractal Geometry of Nature* (Freeman, New York, 1982).

[2] J. Yuan, A. H. E. Müller, K. Matyjaszewski, and S. S. Sheiko, *Polymer Science: A Comprehensive Reference, 10 Volume Set* (Elsevier, Amsterdam, 2012), Vol. 6, pp. 199–264.

[3] G. Grüner, Rev. Mod. Phys. **60**, 1129 (1988).

[4] P. Monceau, Adv. Phys. **61**, 325 (2012).

[5] M. D. Randle, A. Lipatov, I. Mansaray, J. E. Han, A. Sinitskii, and J. P. Bird, Appl. Phys. Lett. **118**, 210502 (2021).

[6] H. Fröhlich, Proc. Roy. Sos. A **223**, 296 (1954).

[7] N. P. Ong and P. Monceau, Phys. Rev. B **16**, 3443 (1977).

[8] P. Monçeau, N. P. Ong, A. M. Portis, A. Meerschaut, and J. Rouxel, Phys. Rev. Lett. **37**, 602 (1976).

[9] S. E. Brown, G. Mozurkewich, and G. Grüner, Phys. Rev. Lett. **52**, 2277 (1984).

[10] M. H. Jensen, P. Bak, and T. Bohr, Phys. Rev. Lett. **50**, 1637 (1983); Phys. Rev. A **30**, 1960 (1984).

[11] T. Bohr, P. Bak, and M. H. Jensen, Phys. Rev. A **30**, 1970 (1984).

[12] P. Bak, Phys. Today **39**(12), 38 (1986).

[13] M. Zaletel, M. Lukin, C. Monroe, C. Nayak, F. Wilczek, and N. Y. Yao, Rev. Mod. Phys. **95**, 031001 (2023).

[14] M. V. Nikitin, S. G. Zybtsev, V. Y. Pokrovskii, and B. A. Loginov, Appl. Phys. Lett. **118**, 223105 (2021).

[15] K. Fujiwara and Y. Niimi, private communication about a SAW experiment where, with the combined use of techniques reported in Refs. [16,17], a 10-μm NbSe₃ wire placed on the LiNbO₃ substrate is irradiated by the SAW with its wavelength being approximately 1 μm, and harmonic and subharmonic Shapiro steps were observed as peaks in the differential resistance. The SAW was generated, via the inverse piezoelectric effect, by applying an ac voltage to comb-shaped electrodes on the piezoelectric substrate LiNbO₃.

[16] K. Fujiwara, S. Iwakiri, M. Watanabe, R. Nakamura, M. Yokoi, K. Kobayashi, and Y. Niimi, Jpn. J. Appl. Phys. **60**, 070904 (2021).

[17] M. Yokoi, S. Fujiwara, T. Kawamura, T. Arakawa, K. Aoyama, H. Fukuyama, K. Kobayashi, and Y. Niimi, Sci. Adv. **6**, eaba1377 (2020).

[18] P. A. Lee, T. M. Rice, and P. W. Anderson, Solid State Commun. **14**, 703 (1974).

[19] L. Liu, C. Zhu, Z. Y. Liu, H. Deng, X. B. Zhou, Y. Li, Y. Sun, X. Huang, S. Li, X. Du, Z. Wang, T. Guan, H. Mao, Y. Sui, R. Wu, J.-X. Yin, J.-G. Cheng, and S. H. Pan, Phys. Rev. Lett. **126**, 256401 (2021).

[20] A. Maeda, Y. Inoue, H. Kitano, S. Savel'ev, S. Okayasu, I. Tsukada, and F. Nori, Phys. Rev. Lett. **94**, 077001 (2005).

[21] V. L. R. Jacques, C. Laulhe, N. Moisan, S. Ravy, and D. Le Bolloch, Phys. Rev. Lett. **117**, 156401 (2016).

[22] R. M. Fleming and C. C. Grimes, Phys. Rev. Lett. **42**, 1423 (1979).

[23] P. Monceau, J. Richard, and M. Renard, Phys. Rev. Lett. **45**, 43 (1980); Phys. Rev. B **25**, 931 (1982).

[24] J. Richard, P. Monceau, and M. Renard, Phys. Rev. B **25**, 948 (1982).

[25] A. Zettl and G. Grüner, Phys. Rev. B **29**, 755 (1984).

[26] S. N. Coppersmith and P. B. Littlewood, Phys. Rev. Lett. **57**, 1927 (1986).

[27] R. E. Thorne, J. S. Hubacek, W. G. Lyons, J. W. Lyding, and J. R. Tucker, Phys. Rev. B **37**, 10055 (1988).

[28] S. Bhattacharya, J. P. Stokes, M. J. Higgins, and R. A. Klemm, Phys. Rev. Lett. **59**, 1849 (1987).

[29] A. A. Middleton, O. Biham, P. B. Littlewood, and P. Sibani, Phys. Rev. Lett. **68**, 1586 (1992).

[30] P. F. Tua and J. Ruvalds, Solid State Commun. **54**, 471 (1985).

[31] H. Matsukawa and H. Takayama, Jpn. J. Appl. Phys. **26**, 601 (1987).

[32] H. Matsukawa and H. Takayama, J. Phys. Soc. Jpn. **56**, 1507 (1987); H. Matsukawa, *ibid.* **56**, 1522 (1987); **57**, 3463 (1988).

[33] A. A. Sinchenko, P. Monceau, and T. Crozes, Phys. Rev. Lett. **108**, 046402 (2012).

[34] A. A. Sinchenko and P. Monceau, Phys. Rev. B **87**, 045105 (2013).

[35] S. A. Nikonov, S. G. Zybtsev, and V. Ya. Pokrovskii, Appl. Phys. Lett. **118**, 253108 (2021).

[36] S. Shapiro, Phys. Rev. Lett. **11**, 80 (1963).

[37] S. Shapiro, A. Janus, and S. Holly, Rev. Mod. Phys. **36**, 223 (1964).

[38] C. C. Grimes and S. Shapiro, Phys. Rev. **169**, 397 (1968).

[39] I. Sokolović, P. Mali, J. Odavić, S. Radosević, S. Y. Medvedeva, A. E. Botha, Y. M. Shukrinov, and J. Tekić, Phys. Rev. E **96**, 022210 (2017).

[40] See Supplemental Material at http://link.aps.org/supplemental/10.1103/PhysRevB.108.L100508 for the origin of the pinning-strength vibration, effects of impurity-position vibration on the CDW sliding, the parameter dependence of the 0/1-step width,

and a perturbative analysis of the mode-locking phenomenon, which includes Refs. [14–17,32,41–47].

[41] M. Mori and S. Maekawa, Appl. Phys. Lett. **122**, 042202 (2023).

[42] Y. Wei and Y. Lei, Phys. Rev. E **106**, 044204 (2022).

[43] H. Fukuyama, J. Phys. Soc. Jpn. **45**, 1474 (1978).

[44] G. Mozurkewich, Phys. Rev. B **42**, 11183 (1990).

[45] R. E. Thorne, W. G. Lyons, J. W. Lyding, J. R. Tucker, and J. Bardeen, Phys. Rev. B **35**, 6360 (1987).

[46] E. Sweetland, C.-Y. Tsai, B. A. Wintner, J. D. Brock, and R. E. Thorne, Phys. Rev. Lett. **65**, 3165 (1990).

[47] J. McCarten, D. A. DiCarlo, and R. E. Thorne, Phys. Rev. B **49**, 10113 (1994).

[48] R. E. Thorne, J. Phys. IV France **131**, 89 (2005).

[49] H. Fukuyama, J. Phys. Soc. Jpn. **41**, 513 (1976).

[50] H. Fukuyama and P. A. Lee, Phys. Rev. B **17**, 535 (1978).

[51] P. A. Lee and T. M. Rice, Phys. Rev. B **19**, 3970 (1979).

[52] Y. Funami and K. Aoyama, JPS Conf. Proc. **38**, 011059 (2023).

[53] B. Hu and J. Tekić, Phys. Rev. E **75**, 056608 (2007).

[54] J. Tekić and Z. Ivić, Phys. Rev. E **83**, 056604 (2011).

[55] S. G. Zybtsev, S. A. Nikonov, V. Ya. Pokrovskii, V. V. Pavlovskiy, and D. Staresinić, Phys. Rev. B **101**, 115425 (2020).

[56] A. Zettl, C. M. Jackson, and G. Gruner, Phys. Rev. B **26**, 5773 (1982).

[57] S. Sridhar, D. Reagor, and G. Gruner, Phys. Rev. Lett. **55**, 1196 (1985).

[58] D. Reagor, S. Sridhar, and G. Gruner, Phys. Rev. B **34**, 2212 (1986).

[59] S. Sridhar, D. Reagor, and G. Gruner, Phys. Rev. B **34**, 2223 (1986).